Check for updates

Received: 19 December 2022 | Accepted: 23 January 2024

DOI: 10.1002/jmv.29455

RESEARCH ARTICLE

JOURNAL OF MEDICAL VIROLOGY WILEY

Innate immune response to SARS-CoV-2 infection contributes to neuronal damage in human iPSC-derived peripheral neurons

Vania Passos[1] | Lisa M. Henkel[2] | Jiayi Wang[1] | Francisco J. Zapatero-Belinchón[3,4,5] | Rebecca Möller[3] | Guorong Sun[1] | Inken Waltl[6] | Talia Schneider[1] | Amelie Wachs[1] | Birgit Ritter[1] | Kai A. Kropp[1] | Shuyong Zhu[1] | Michela Deleidi[7,8] | Ulrich Kalinke[4,6] | Thomas F. Schulz[1,4] | Günter Höglinger[2,4] | Gisa Gerold[3,4,5,9] | Florian Wegner[2] | Abel Viejo-Borbolla[1,4]

[1]Hannover Medical School, Institute of Virology, Hannover, Germany

[2]Department of Neurology, Hannover Medical School, Hannover, Germany

[3]University of Veterinary Medicine Hannover, Foundation, Hannover, Germany

[4]Cluster of Excellence-Resolving Infection Susceptibility (RESIST), Hannover Medical School, Hannover, Germany

[5]Department of Clinical Microbiology, Umeå University, Umeå, Sweden

[6]Institute for Experimental Infection Research, TWINCORE, Centre for Experimental and Clinical Infection Research, A Joint Venture between the Helmholtz Centre for Infection Research and the Hannover Medical School, Hannover, Germany

[7]Center of Neurology, Hertie Institute for Clinical Brain Research, University of Tübingen, Tübingen, Germany

[8]German Center for Neurodegenerative Diseases (DZNE), Tübingen, Germany

[9]Wallenberg Centre for Molecular Medicine (WCMM), Umeå University, Umeå, Sweden

Correspondence

Abel Viejo-Borbolla, Hannover Medical School, Institute of Virology, Carl-Neuberg Strasse 1, Hannover, Germany.
Email: viejo-borbolla.abel@mh-hannover.de

Present addresses

Francisco J. Zapatero-Belinchón, Gladstone Institutes, San Francisco, California, USA.

Shuyong Zhu, Beyotime Biotech Inc., Haimen, Jiangsu, China.

Funding information

Chinese Government Scholarship; Deutsche Forschungsgemeinschaft

Abstract

Severe acute respiratory coronavirus 2 (SARS-CoV-2) causes neurological disease in the peripheral and central nervous system (PNS and CNS, respectively) of some patients. It is not clear whether SARS-CoV-2 infection or the subsequent immune response are the key factors that cause neurological disease. Here, we addressed this question by infecting human induced pluripotent stem cell-derived CNS and PNS neurons with SARS-CoV-2. SARS-CoV-2 infected a low number of CNS neurons and did not elicit a robust innate immune response. On the contrary, SARS-CoV-2 infected a higher number of PNS neurons. This resulted in expression of interferon (IFN) λ1, several IFN-stimulated genes and proinflammatory cytokines. The PNS neurons also displayed alterations characteristic of neuronal damage, as increased levels of sterile alpha and Toll/interleukin receptor motif-containing protein 1, amyloid precursor protein and α-synuclein, and lower levels of

This is an open access article under the terms of the Creative Commons Attribution-NonCommercial License, which permits use, distribution and reproduction in any medium, provided the original work is properly cited and is not used for commercial purposes.
© 2024 The Authors. *Journal of Medical Virology* published by Wiley Periodicals LLC.

cytoskeletal proteins. Interestingly, blockade of the Janus kinase and signal transducer and activator of transcription pathway by Ruxolitinib did not increase SARS-CoV-2 infection, but reduced neuronal damage, suggesting that an exacerbated neuronal innate immune response contributes to pathogenesis in the PNS. Our results provide a basis to study coronavirus disease 2019 (COVID-19) related neuronal pathology and to test future preventive or therapeutic strategies.

KEYWORDS

interferon, iPSC-derived peripheral neurons, JAK/STAT, neuronal damage, SARM1, SARS-CoV-2

1 | INTRODUCTION

Severe acute respiratory coronavirus 2 (SARS-CoV-2) causes coronavirus disease 2019 (COVID-19). Clinical studies indicate that some patients infected with SARS-CoV-2 develop neurological disease in the central and peripheral nervous systems (CNS and PNS, respectively).[1–7] Diseases associated with the PNS occurring after SARS-CoV-2 infection include nerve pain, Guillain–Barré syndrome, myasthenia gravis, neurosensory disorders, and peripheral neuropathy.[4,8–13] Moreover, many individuals with long COVID-19 suffer from neurological disorders including brain fog and cognitive impairment, implying the persistence of neurological damage or even progression to neurodegenerative diseases.[2,14–16] Interestingly, some long COVID-19 patients with neurological symptoms have increased loss of small nerve fibers in the cornea[17] and peripheral neuropathy, probably due to an exacerbated immune response to infection.[18]

Currently, it is not clear whether neurological diseases in COVID-19 patients are due to direct effects of viral infection of the nervous system or to an indirect impact of the immune response. SARS-CoV-2 RNA genome, transcripts, and antigens were detected in the cerebrospinal fluid and brains of some, but not all, COVID-19 patients that developed neurological abnormalities following infection.[19–24] It has been suggested that a dysregulation of the immune response, including the induction of a cytokine storm, is responsible for neurological complications during COVID-19.[9,25–29]

To investigate the underlying mechanisms of neurological symptoms following SARS-CoV-2 infection, several groups employed human neurons and neuronal models derived from stem cells such as human iPSC-derived CNS neurons and brain organoids.[23,30–36] However, there are differences regarding the efficiency of viral replication in human CNS. Moreover, there are discrepancies on the type of CNS cells—neurons, epithelial, glial cells—that are productively infected.[23,30–36] Most of the studies focused on neurons of the CNS rather than on those of the PNS. In one of the few studies addressing SARS-CoV-2 infection of human PNS neurons, the authors showed efficient infection of human embryonic stem cell-derived peripheral neurons and changes in the expression of chemosensory genes.[37]

Neurons can detect viruses through pattern recognition receptors as well as express and respond to interferon (IFN) to combat virus infection.[36,38–44] Neurons also respond to viral infections by inducing axonal degeneration, apoptosis, and autophagy, although the latter can also be proviral.[45–50] Under certain circumstances, the innate and intrinsic neuronal responses to viral infection can lead to neurodegenerative processes, for example, through the unfolded protein response (UPR)[51,52] and activation of sterile alpha and Toll/interleukin (IL) receptor motif-containing protein 1 (SARM1), a protein that triggers neurite degeneration.[50,53–55]

Here, we addressed the impact of SARS-CoV-2 infection and the subsequent innate and intrinsic immune responses on the induction of neuronal damage using human iPSC-derived CNS and PNS neurons. Interestingly, human iPSC-derived neurons with characteristics of the PNS were much more permissive to SARS-CoV-2 than those resembling neurons of the CNS. This was accompanied by increased type III IFN response, loss of cytoskeleton proteins (β-III-tubulin and microtubule-associated protein 2, MAP2), as well as gene and protein expression profiles characteristic of neuronal damage. Interestingly, inhibition of the Janus kinase and signal transducer and activator of transcription (JAK/STAT) pathway by Ruxolitinib reduced neurite damage. Our results suggest that there are important differences in the way that CNS and PNS neurons respond to SARS-CoV-2 infection and link the innate immune response with neuronal damage in human PNS neurons.

2 | METHODS

2.1 | Cells and viruses

Sensory neurons and striatal medium spiny neurons (MSNs) were derived from iPSC and maintained as previously described.[56,57] To differentiate sensory neurons, we employed small molecule derived neuronal precursor cells (smNPCs) generated from cord blood-derived iPSC.[58] The MSNs were differentiated from a control iPSC line.[59] The Vero76 cell line is a derivative of Vero cells, kidney epithelial cells from African green monkeys. Vero76 cells were cultured with DMEM supplemented with 10% fetal calf serum (FCS), 10 mM 4-(2-hydroxyethyl)-1-piperazineethanesulfonic acid (HEPES), and 1% of penicillin/streptomycin (Pen/Strep) in a humidified incubator at 37°C and with 5% CO_2. To prepare virus stocks, Vero76

10969071, 2024, 2, Downloaded from https://onlinelibrary.wiley.com/doi/10.1002/jmv.29455 by Deutsches Zentrum Für Neurologie, Wiley Online Library on [19/02/2024]. See the Terms and Conditions (https://onlinelibrary.wiley.com/terms-and-conditions) on Wiley Online Library for rules of use; OA articles are governed by the applicable Creative Commons License

cells were incubated with infection medium (DMEM supplemented with 2% FCS, 10 mM HEPES, and 1% Pen/Strep) containing SARS-CoV-2 Beta strain at an multiplicity of infection (MOI) of 0.01 plaque forming units (PFU)/cell for 48–72 h in a humidified incubator at 37°C and with 5% CO_2. Cell supernatant (SN) was collected and centrifuged at 450*g* for 5 min. Virus aliquots were stored at −80°C.

To determine the virus titer, we performed a plaque assay in VeroB4 cells, a derivative of Vero cells, which were maintained in a humidified incubator at 37°C and with 5% CO_2. 7×10^5 VeroB4 cells/well grown in six-well plates were inoculated with 10-fold serial dilutions of the virus in infection medium (1 x MEM, 5% FCS, 25 mM HEPES, 0.5% Glutamax) for 1 h at 37°C and 5% CO_2. During inoculation, the plates were rocked gently every 15 min to prevent the cells from drying out. The inoculum was then replaced by 2 mL of carboxymethyl cellulose (CMC) overlay (1 x MEM, 1% CMC, 5% FCS, 0.37% $NaHCO_3$, 25 mM HEPES) per well. After an incubation period of 3 days at 37°C and 5% CO_2, the CMC overlay was removed and the cells washed twice with PBS. The cells were fixed with 10% formalin for 30 min at room temperature and the plates air-dried under a chemical fume hood. The plaques were visualized by applying 0.05% (w/v) crystal violet solution in 20% methanol for 20 min and rinsing the cells with ddH_2O. The viral titer, expressed as PFU per mL, was calculated using the formula PFU/mL = Number of plaques/infection volume × $10^{dilution}$.

2.2 | Infection of iPSC-derived human neurons and Vero cells

To test for productive infection: 70 days differentiated MSNs were infected with SARS-CoV-2 β strain at an MOI of 0.01–1. One hour after the addition of the virus (humidified incubator at 37°C and with 5% CO_2), the inoculum was removed and 1:1 DMEM/F12 medium and Neurobasal medium supplemented with XN2, XB27, 1% of Pen/Strep/glutamine, 10 ng/mL of BDNF, 10 ng/mL GDNF, 25 ng/mL NGF, and 50 µM dbcAMP was added to the cells. Cells were incubated in a humidified incubator at 37°C and with 5% CO_2 for 24 and 48 h; Vero76 cells were infected with SARS-CoV-2 Beta strain at an MOI of 0.01 (or with UV-inactivated SARS-CoV-2 β strain, kindly provided by Thomas Pietschmann, Experimental Virology, Twincore) for 72 h and maintained with DMEM supplemented with 2% FCS, 10 mM HEPES, and 1% of Pen/Strep.

For the remaining experiments, differentiated CNS and PNS neurons were infected with SARS-CoV-2 Beta strain at an MOI of 0.01 for 72 h, without removal of the inoculum after 1 h. MSNs were incubated in 1:1 DMEM/F12 medium and Neurobasal medium supplemented with XN2, XB27, 1% of Pen/Strep/glutamine, 10 ng/mL BDNF, 10 ng/mL GDNF, 25 ng/mL NGF, and 50 µM dbcAMP; PNS neurons were incubated in 1:1 DMEM/F12 medium and Neurobasal medium supplemented with 0.5% N2, 1% B27, 1% of Pen/Strep/glutamine, 10 ng/mL BDNF, 10 ng/mL GDNF, and 25 ng/mL NGF. To determine the role of the JAK/STAT pathway, we added 10 µM of Ruxolitinib (Adipogen) 18 h before infection. Mock-infected cells were treated as infected ones without addition of the virus.

2.3 | Multiplex assay

SN of SARS-CoV-2- and mock-infected neurons, pretreated with 10 µm Ruxolitinib or mock-treated, was collected. Virus was inactivated by incubating the SN with 7.5% $NaHCO_3$ on ice for 10 min. Then, the SN was incubated with 0.1% of β-propiolactone (BPL) for 72 h at 4°C. BPL was hydrolyzed by incubating the SN at 37°C for 2 h. The SN was then stored at −20°C until use. To measure the cytokines/chemokines present in the SN, we chose the LEGENDplex™ bead-based immunoassay and quantified the following cytokines/chemokines from the panels COVID-19 Cytokine Storm 1 (CCL2, CCL5, CXCL10, IFN-γ, IL-10, IL-6; Biolegend cat. No. 741088) and Human Neurodegeneration Biomarkers 1 (neurofilament light [NFL], Tau, α-synuclein; Biolegend cat. No. 741197). The assay was performed following the manufacturer's instructions. We used the SN without applying any dilution factor. Data acquisition was achieved as advised in the manufacturer's manual. Data analysis was performed using the LEGENDplex™ Data Analysis Software. Protein concentration (pg/mL) was measured as the predicted concentration relative to the standards of each panel. Error bars represent standard deviation of the arithmetic mean from three independent experiments.

2.4 | Statistical analysis

The *p* value was calculated using GraphPad Prism by performing one-way ANOVA followed by Dunnetts' multiple comparison posttest. Each gene was analyzed separately and group comparisons were performed. In most of the cases Mock untreated control was set as 1. For most of the data, logarithmic transformation was performed to reinsure Gaussian distribution. Error bars represent standard deviation of the arithmetic mean from three independent experiments. Statistical significance was shown as $*p < 0.03$; $**p < 0.002$; $***p < 0.0002$; $****p < 0.0001$; ns, not significant.

3 | RESULTS

To determine the effect of SARS-CoV-2 infection in PNS and CNS neurons, we employed protocols developed in our laboratories to differentiate human iPSC into neurons with characteristics of sensory and striatal MSN (schematic depiction in Figure 1A,B).[56,57] For the sake of clarity, we will refer to the sensory neurons and MSN as PNS and CNS neurons, respectively.

3.1 | iPSC-derived human CNS and PNS neurons express low levels of SARS-CoV-2 receptors and entry factors

SARS-CoV-2 cell entry normally requires processing of the S protein by transmembrane protease, serine 2 (TMPRSS2), followed by binding to ACE2.[60,61] Neuropilin-1 (Nrp-1) is thought

10969071, 2024, 2, Downloaded from https://onlinelibrary.wiley.com/doi/10.1002/jmv.29455 by Deutsches Zentrum Für Neurologie, Wiley Online Library on [19/02/2024]. See the Terms and Conditions (https://onlinelibrary.wiley.com/terms-and-conditions) on Wiley Online Library for rules of use; OA articles are governed by the applicable Creative Commons License

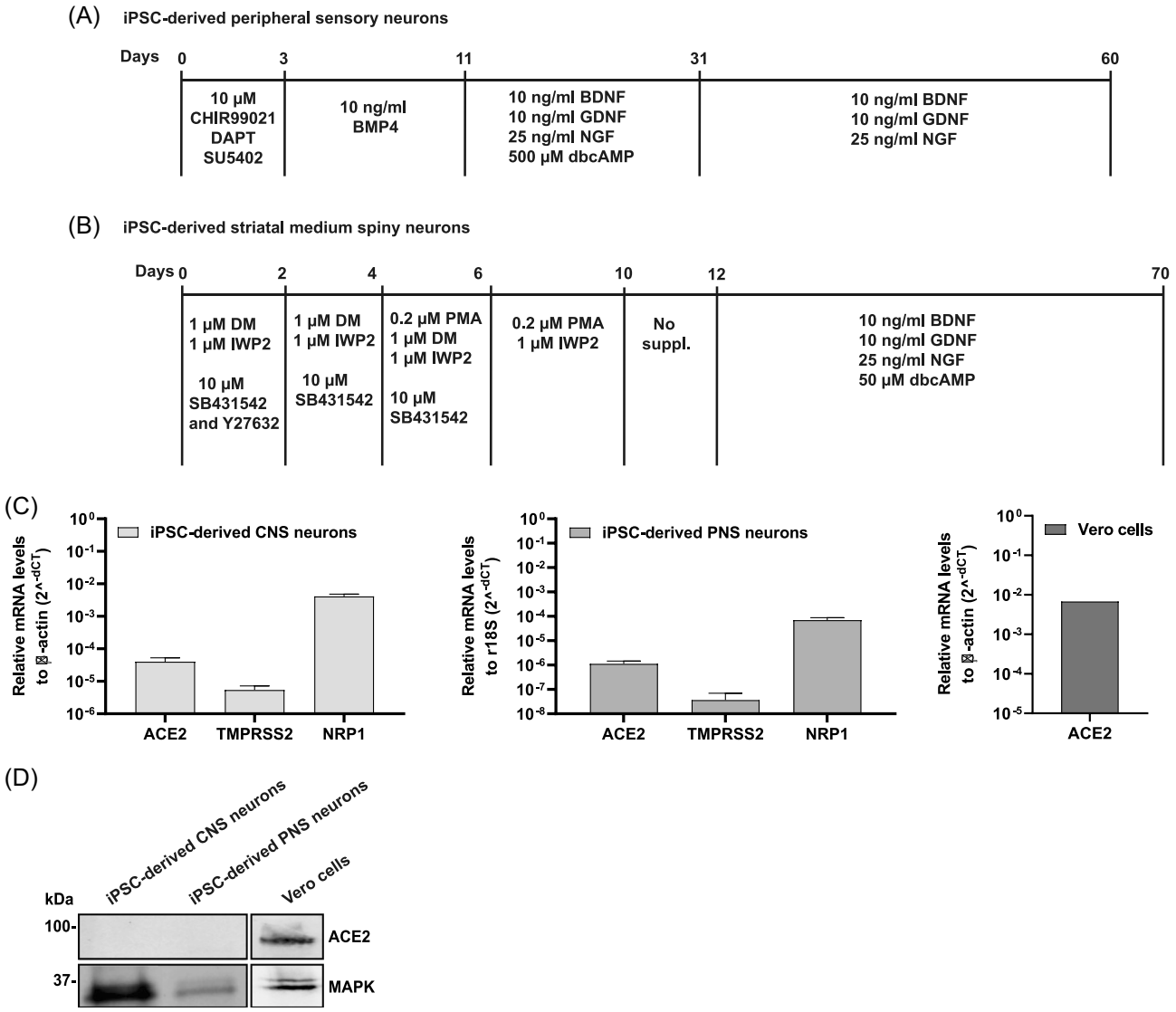

FIGURE 1 Differentiation of human iPSC-derived CNS and PNS neurons, and their expression profiles of SARS-CoV-2 receptors and entry factors. (A, B) PNS (A) and CNS (B) neurons were differentiated from iPSC adding the indicated supplements at the corresponding time points.[56,57] (C) Graphs showing relative expression of *ACE2*, *TMPRSS2*, and *NRP1* in iPSC-derived CNS neurons (left) and PNS neurons (middle) and that of *ACE2* in Vero76 cells (right). Gene expression was set relative to β-actin or 18S. Error bars represent standard deviation of the arithmetic mean from three independent experiments. (D) Western blot analysis showing detection of ACE2 and MAPK in cell lysates of iPSC-derived CNS and PNS neurons and Vero76 cells. One representative blot, out of three independent ones, is shown. BDNF, brain-derived neurotrophic factor; BMP4, bone morphogenetic protein 4; CNS, central nervous system; DAPT, γ-secretase inhibitor; dbcAMP, dibutyryl cyclic adenosine monophosphate; DM, dorsomorphin; GDNF, glial cell line-derived neurotrophic factor; iPSC, induced pluripotent stem cells; IWP2, Wnt antagonist 2; NGF, nerve growth factor; PMA, purmorphamine; PNS, peripheral nervous system; SARS-CoV-2, severe acute respiratory coronavirus 2; SB431542, TGF-β inhibitor; Y27632, rock inhibitor.

to facilitate SARS-CoV-2 infection[62,63] and mediates entry into human astrocytes in brain organoids.[64] Therefore, we determined the mRNA levels of *ACE2*, *TMPRSS2*, and *Nrp-1* using quantitative PCR. Both neuronal subtypes expressed low mRNA levels of *ACE2*, *TMPRSS2*, and *Nrp-1* and no detectable ACE2 protein, while Vero76 cells, used to prepare SARS-CoV-2 stocks, expressed higher ACE2 mRNA and protein (Figure 1C,D).

3.2 | SARS-CoV-2 infects a low number of iPSC-derived human CNS neurons and does not trigger a strong innate immune response

We addressed whether SARS-CoV-2 infected iPSC-derived human CNS neurons despite the low expression level of known SARS-CoV-2 entry factors. Infection of CNS neurons with SARS-CoV-2 Beta strain

10969071, 2024, 2, Downloaded from https://onlinelibrary.wiley.com/doi/10.1002/jmv.29455 by Deutsches Zentrum Für Neurologie, Wiley Online Library on [19/02/2024]. See the Terms and Conditions (https://onlinelibrary.wiley.com/terms-and-conditions) on Wiley Online Library for rules of use; OA articles are governed by the applicable Creative Commons License

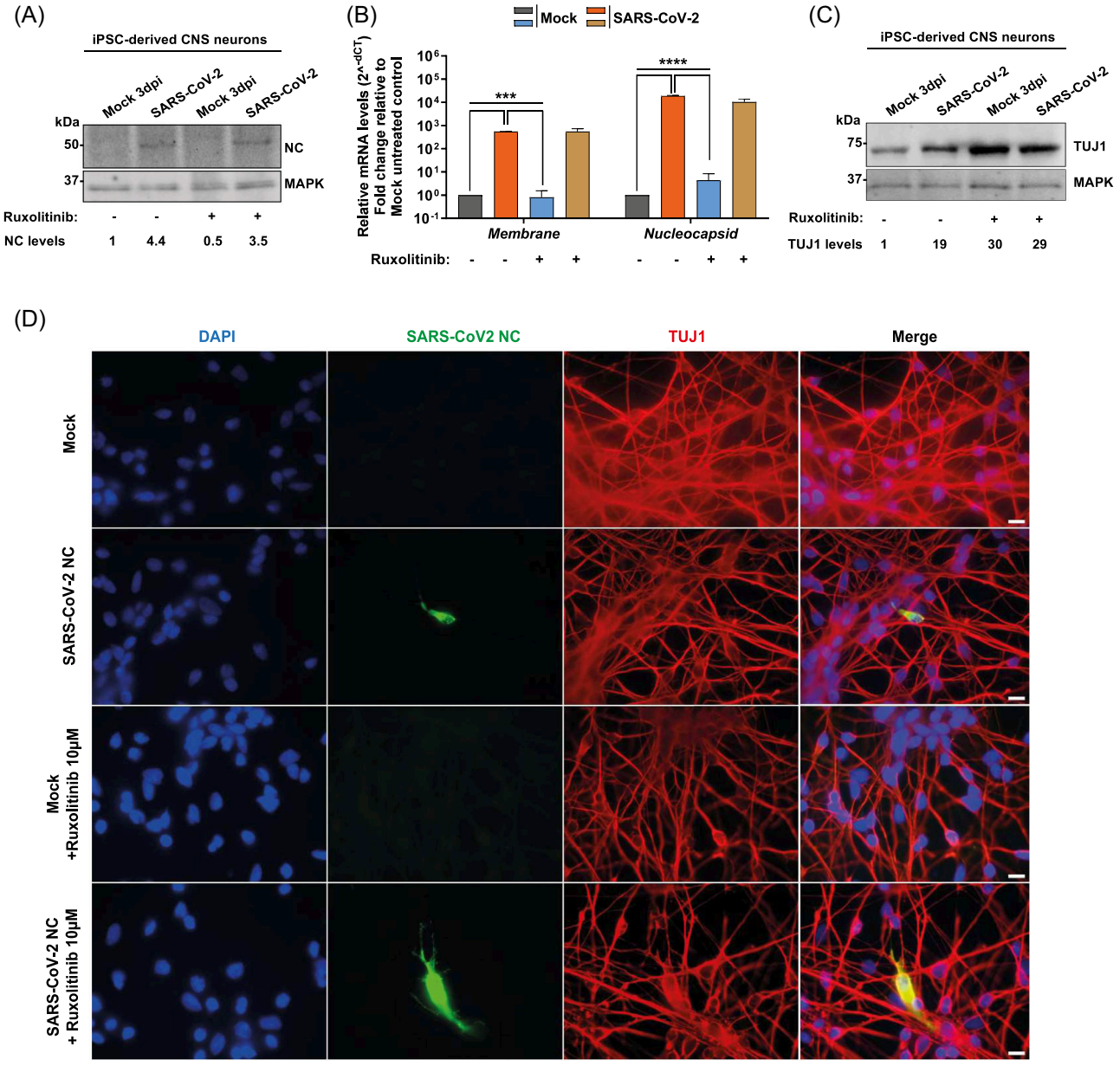

FIGURE 2 SARS-CoV-2 infects CNS neurons with low efficiency without eliciting a robust IFN and ISG response. (A) Western blot analysis showing SARS-CoV-2 NC and MAPK in CNS neurons lysed at 3 dpi. NC levels relative to MAPK were measured with ImageJ. Shown is a representative blot from three independent experiments. (B) Graphs showing relative expression of SARS-CoV-2 *Membrane* and *Nucleocapsid* mRNA in CNS neurons at 3 dpi. (C) Immunoblot showing TUJ1 and MAPK in cell lysates of CNS neurons at 3 dpi. TUJ1 levels relative to MAPK were measured using ImageJ. One representative blot, out of three independent ones, is shown. (D) Immunofluorescence of CNS neurons fixed at 3 dpi. The cells were stained with anti-SARS-CoV-2 NC, anti-TUJ1, and DAPI. Scale bar = 20 µm; amplification: ×100. (E, G, I) Graphs showing relative expression of host genes in CNS neurons at 3 dpi. (F) Graph showing protein concentrations of several cytokines in supernatants (SN) obtained from CNS neurons at 3 dpi determined by ELISA. (H) Immunoblot to detect ISG15 and MAPK in cell lysates of CNS neurons. Relative ISG15 levels were measured using ImageJ. A representative blot, out of three independent ones, is shown. (J) Graph showing protein concentrations of several cytokines in SN obtained from CNS neurons at 3 dpi determined by cytometric bead array multiplex analysis. In all immunoblots, the numbers below the blot represent the fold change to mock-infected, untreated control. In all graphs showing gene expression, this was quantified by RT-qPCR and set relative to β-actin. Fold-change is relative to mock-infected, untreated control. In all graphs, error bars represent standard deviation of the arithmetic mean from three independent experiments. Statistical analyses for all experiments were determined using one-way ANOVA followed by the Dunnetts multiple comparison posttest. $^{*}p < 0.03$; $^{**}p < 0.002$; $^{***}p < 0.0002$; $^{****}p < 0.0001$; not significant comparisons are not indicated. CNS, central nervous system; IFN, interferon; SARS-CoV-2, severe acute respiratory coronavirus 2.

10969071, 2024, 2, Downloaded from https://onlinelibrary.wiley.com/doi/10.1002/jmv.29455 by Deutsches Zentrum Für Neurodeg, Wiley Online Library on [19/02/2024]. See the Terms and Conditions (https://onlinelibrary.wiley.com/terms-and-conditions) on Wiley Online Library for rules of use; OA articles are governed by the applicable Creative Commons License

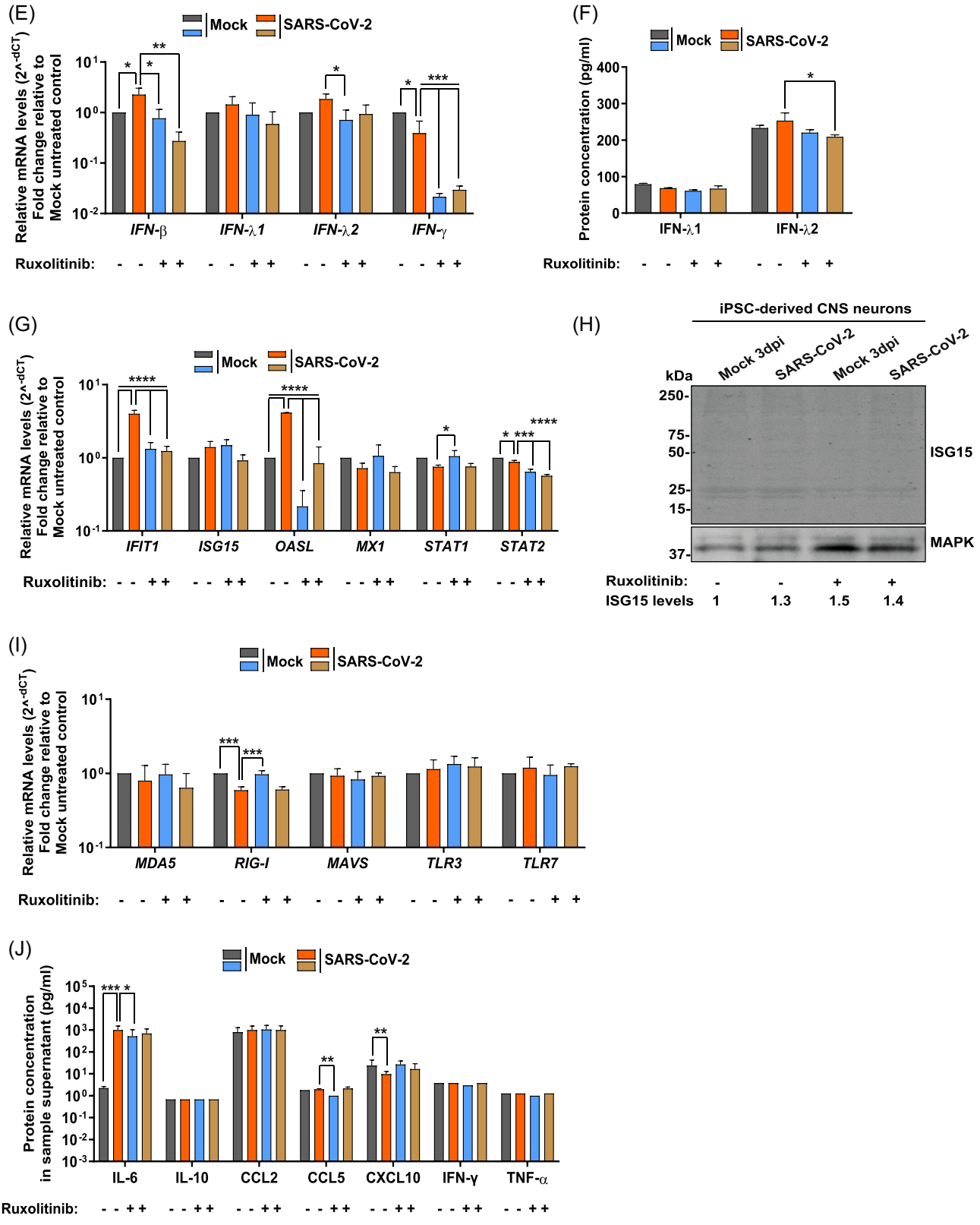

FIGURE 2 (Continued).

at an MOI of 0.01 led to low expression of nucleocapsid (NC) protein compared to the results obtained with infected Vero76 cells (Figure 2A and Figure S1A). We could not detect NC protein in Vero76 cells infected with UV-inactivated SARS-CoV-2, suggesting that the detected protein corresponded to newly expressed NC (Figure S1A). We also detected *NC* and *Membrane* transcripts in CNS neurons infected with SARS-CoV-2 (Figure S1B). SARS-CoV-2 mRNA expression increased in a time and MOI dependent manner

10969071, 2024, 2, Downloaded from https://onlinelibrary.wiley.com/doi/10.1002/jmv.29455 by Deutsches Zentrum Für Neurologie, Wiley Online Library on [19/02/2024]. See the Terms and Conditions (https://onlinelibrary.wiley.com/terms-and-conditions) on Wiley Online Library for rules of use; OA articles are governed by the applicable Creative Commons License

(Figure S1B). These results suggested that SARS-CoV-2 replicated in CNS neurons, although at low efficiency. To address whether the neuronal innate immune response could limit virus replication, we blocked the JAK/STAT pathway with Ruxolitinib before exposure of CNS neurons to SARS-CoV-2. Interestingly, Ruxolitinib did not modulate the infection efficiency of SARS-CoV-2 at the translational or transcriptional level (Figure 2A,B).

Costaining of the NC protein and β-III-tubulin (TUJ1) indicated that only a few neurons were infected (Figure 2D). The number of NC positive CNS neurons was low and dispersed in the culture. We did not detect a clear cytopathic effect and the protein level of the cytoskeleton protein β-III-tubulin did not decrease upon SARS-CoV-2 infection (Figure 2C). Instead, we observed more β-III-tubulin compared to the mock-infected cells, suggesting no degradation of this cytoskeletal protein upon infection of CNS neurons. Inhibition of the JAK/STAT pathway resulted in higher β-III-tubulin level in CNS neurons that were either mock- or SARS-CoV-2-infected (Figure 2C). Overall, these results show that SARS-CoV-2 infects a limited number of iPSC-derived human CNS neurons, which do not appear to be severely damaged by the presence of the virus. Moreover, they suggest that the activity of the JAK/STAT pathway did not influence the level of infection.

We then addressed whether CNS neurons responded to infection with SARS-CoV-2 by expressing IFN and interferon-stimulated genes (ISGs). Infection with SARS-CoV-2 increased the expression of type I (*IFN-β*) and type III IFN (*IFN-λ2*) and decreased that of *IFN-γ* (Figure 2E), but IFN-λ2 protein levels did not significantly increase (Figure 2F) and IFN-γ protein levels did not change (Figure 2J and Figure S3A). Expression of most ISGs analyzed did not change with infection, with the exception of IFN induced protein with tetratricopeptide repeats 1 (*IFIT1*) and 2′-5′-Oligoadenylate synthetase like (*OASL*) that were increased, and *STAT2* that was slightly decreased (Figure 2G). There was no detectable ISG15 (Figure 2H). Ruxolitinib decreased the expression of *IFN-β*, *IFN-λ2*, *IFN-γ*, *IFIT1*, and *OASL* in SARS-CoV-2 infected neurons, indicating that the treatment was effective (Figure 2E,G).

We then investigated the expression level of pattern recognition receptors known to be involved in SARS-CoV-2 recognition, namely melanoma differentiation-associated protein 5 (*MDA-5*), retinoic acid-inducible gene I (*RIG-I*), mitochondrial antiviral-signaling protein (*MAVS*), and Toll-like receptor 3 and 7 (*TLR3* and *TLR7*, respectively). Interestingly, *RIG-I* was decreased in the presence of SARS-CoV-2 (Figure 2I).

We then determined the level of cytokines present in the SN of mock- and SARS-CoV-2-infected CNS neurons in the absence and presence of Ruxolitinib. The level of CXCL10 was lower in infected cells and, with the exception of IL-6, none of the analyzed cytokines increased during SARS-CoV-2 infection (Figure 2J), suggesting that CNS neurons were not in a state of inflammation at 3 dpi with SARS-CoV-2. Surprisingly, inhibition of the JAK/STAT pathway resulted in high IL-6 protein levels in both mock- and SARS-CoV-2-infected CNS neurons (Figure 2J).

Altogether, SARS-CoV-2 infected CNS neurons with low efficiency and did not elicit a robust innate immune response.

3.3 | SARS-CoV-2 does not induce endoplasmic reticulum (ER) stress nor neuronal damage in iPSC-derived CNS neurons

The UPR pathway controls ER homeostasis and becomes activated upon induction of ER stress. Chronic activation of the UPR can lead to neurodegenerative diseases.[65–67] We investigated whether SARS-CoV-2 infection induced ER stress in CNS neurons by determining the expression level of activating transcription factor 4 (*ATF4*), CCAAT/enhancer-binding protein homologous protein (*CHOP*), binding immunoglobulin protein (*BiP*), and 94 kDa glucose regulated protein (*GRP94*). There were no signs of ER stress, such as upregulation of *ATF4* and *CHOP*, neither downregulation of *BiP* upon infection of CNS neurons compared to the mock-treated cells (Figure 3A). Interestingly, BiP expression was significantly increased both at the transcriptional and translational level in the CNS neurons exposed to SARS-CoV-2 (Figure 3A,B). Moreover, both SARS-CoV-2 infection and Ruxolitinib treatment reduced the expression of *GRP94* (Figure 3A). Overall, these results suggest that CNS neurons responded to SARS-CoV-2 without severe dysregulation of the UPR pathway.

We also investigated the impact of SARS-CoV-2 infection on the expression of several genes involved in neurodegeneration such as *SARM1*, nicotinamide mononucleotide adenylyltransferase 2 (*NMNAT2*), β-amyloid precursor protein (*APP*), and the structural protein *MAP2*. SARM1 is essential and sufficient to trigger neurite degeneration, and becomes active due to depletion of NMNAT2.[53,55,68] CNS neurons infected with SARS-CoV-2 did not show patterns of axonal degeneration, but rather axonal survival, with increased transcript levels of *NMNAT2* and *MAP2*, reduced expression of *SARM1* and no changes in *APP* levels compared to the mock-treated CNS neurons (Figure 3C,D). Addition of Ruxolitinib further increased mRNA of *NMNAT2* cells and restored *SARM1* levels to those observed in mock-infected cells (Figure 3C). Interestingly, Ruxolitinib treatment reduced SARM1 protein levels (Figure 3D). Addition of Ruxolitinib also increased *MAP2* transcripts in both mock- and SARS-CoV-2-infected cells compared to the samples without the inhibitor, while mRNA levels of *APP* did not significantly change (Figure 3C). Moreover, the protein levels of tubulin associated unit (Tau) and NFL chain did not change upon infection and treatment with Ruxolitinib, while α-synuclein secretion was lower in the presence of the virus, regardless of the presence of Ruxolitinib (Figure 3E).

Overall, we demonstrated that infection of human iPSC-derived CNS neurons with SARS-CoV-2 increased mRNA and protein expression of BiP, a central regulator of ER function.[69] Moreover, we observed gene and protein expression profiles associated with neuronal survival and not with neuronal damage.

3.4 | SARS-CoV-2 productively infects iPSC-derived human PNS neurons and induces a type III IFN response

There are only a few studies on infection of PNS neurons with SARS-CoV-2. Therefore, we infected human iPSC-derived PNS neurons with

10969071, 2024, 2, Downloaded from https://onlinelibrary.wiley.com/doi/10.1002/jmv.29455 by Deutsches Zentrum Für Neurologie, Wiley Online Library on [19/02/2024]. See the Terms and Conditions (https://onlinelibrary.wiley.com/terms-and-conditions) on Wiley Online Library for rules of use; OA articles are governed by the applicable Creative Commons License

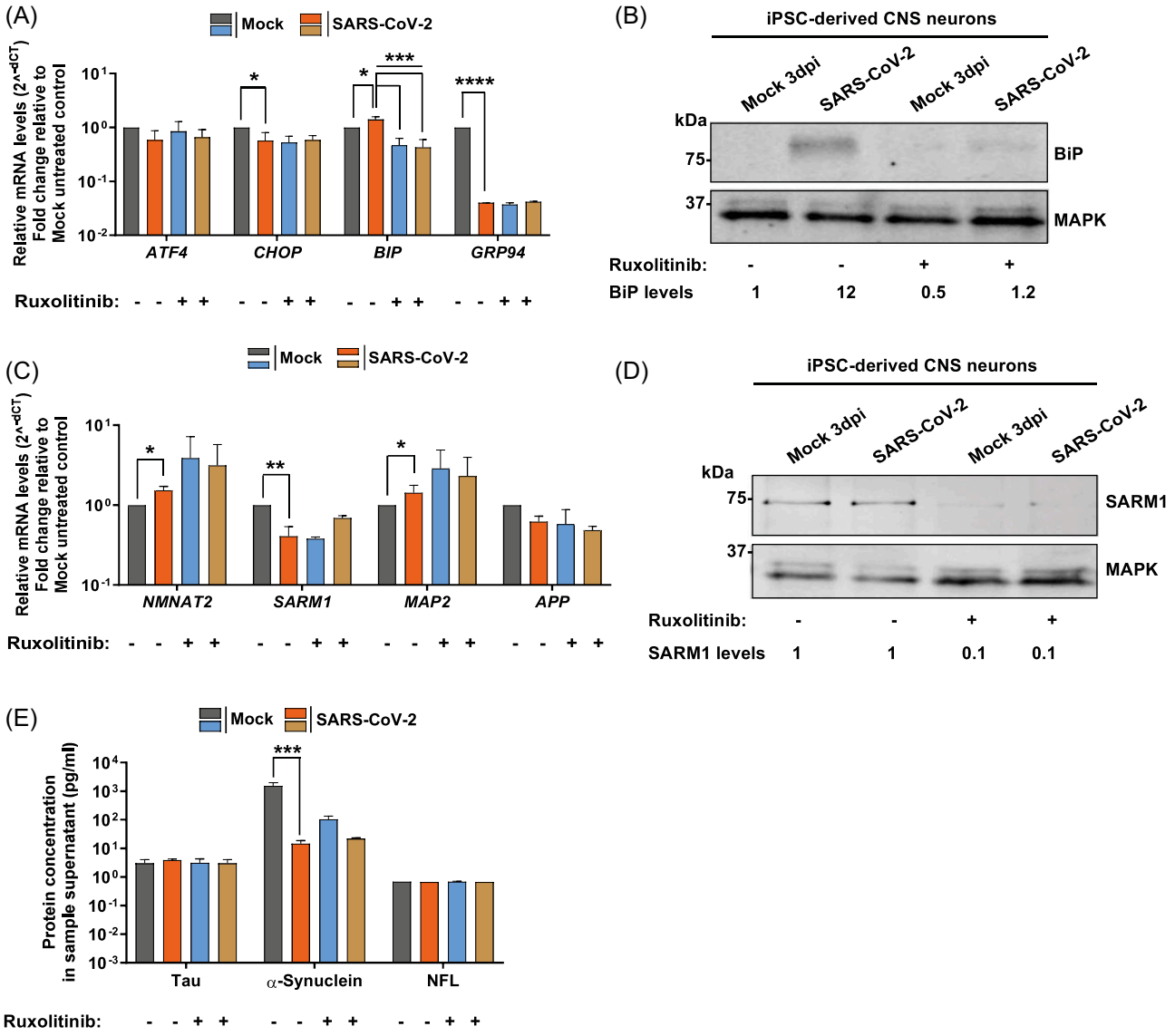

FIGURE 3 SARS-CoV-2 infected CNS neurons do not show cytopathic expression patterns. (A, C) Graphs showing relative expression of host genes in CNS neurons at 3 dpi. Gene expression was quantified by RT-qPCR and set relative to β-actin. Fold-change is relative to mock-infected, untreated control. (B, D) Immunoblots showing BiP (B), SARM1 (D), and MAPK (B, D) in cell lysates of CNS neurons obtained at 3 dpi. BiP and SARM1 levels were measured relative to MAPK using ImageJ. The numbers at the bottom of the blot represent the fold change to mock-treated control. One representative blot, out of three independent ones, is shown. (E) Protein concentrations of released Tau, α-synuclein, and Neurofilament L (NFL) determined by cytometric bead array multiplex analysis. In all graphs, error bars represent standard deviation of the arithmetic mean from three independent experiments. Statistical analyses for all experiments were determined using one-way ANOVA followed by the Dunnetts multiple comparison posttest. *$p < 0.03$; **$p < 0.002$; ***$p < 0.0002$; ****$p < 0.0001$; not significant comparisons are not indicated. CNS, central nervous system; SARS-CoV-2, severe acute respiratory coronavirus 2.

SARS-CoV-2 employing the same conditions as for the iPSC-derived CNS neurons. We observed similar NC protein amounts in the presence or absence of Ruxolitinib (Figure 4A). We also detected mRNA expression of *Membrane* and *NC*, and transcripts of the former were moderately reduced in the presence of Ruxolitinib (Figure 4B). Infection of PNS neurons was productive since SN collected from these cells at 72 h postinfection formed infectious plaques in VeroB4 cells (Figure S2). The number of infected PNS neurons was higher than when we infected CNS neurons (Figure 4D). We also observed cytopathic effects in the cells, including lack of β-III-tubulin staining within some neurites, suggesting that neuronal damage took place (Figure 4D, yellow box). Neurons treated with Ruxolitinib had less cytopathic effect (Figure 4D). Moreover, there was less total β-III-tubulin protein upon SARS-CoV-2 infection compared to the mock-treated neurons, and a reversion to mock levels upon inhibition of the JAK/STAT pathway (Figure 4C). These results suggest that iPSC-derived PNS neurons undergo some degree of neuronal damage upon SARS-CoV-2 infection, which is inhibited or delayed to some extent through suppression of the JAK/STAT pathway.

Next, we explored the effect of infection and inhibition of the JAK/STAT pathway in the expression of genes involved in the innate immune response during SARS-CoV-2 infection of PNS neurons. Interestingly, SARS-CoV-2 elicited a type III IFN response in PNS

10969071, 2024, 2, Downloaded from https://onlinelibrary.wiley.com/doi/10.1002/jmv.29455 by Deutsches Zentrum Für Neurodeg, Wiley Online Library on [19/02/2024]. See the Terms and Conditions (https://onlinelibrary.wiley.com/terms-and-conditions) on Wiley Online Library for rules of use; OA articles are governed by the applicable Creative Commons License

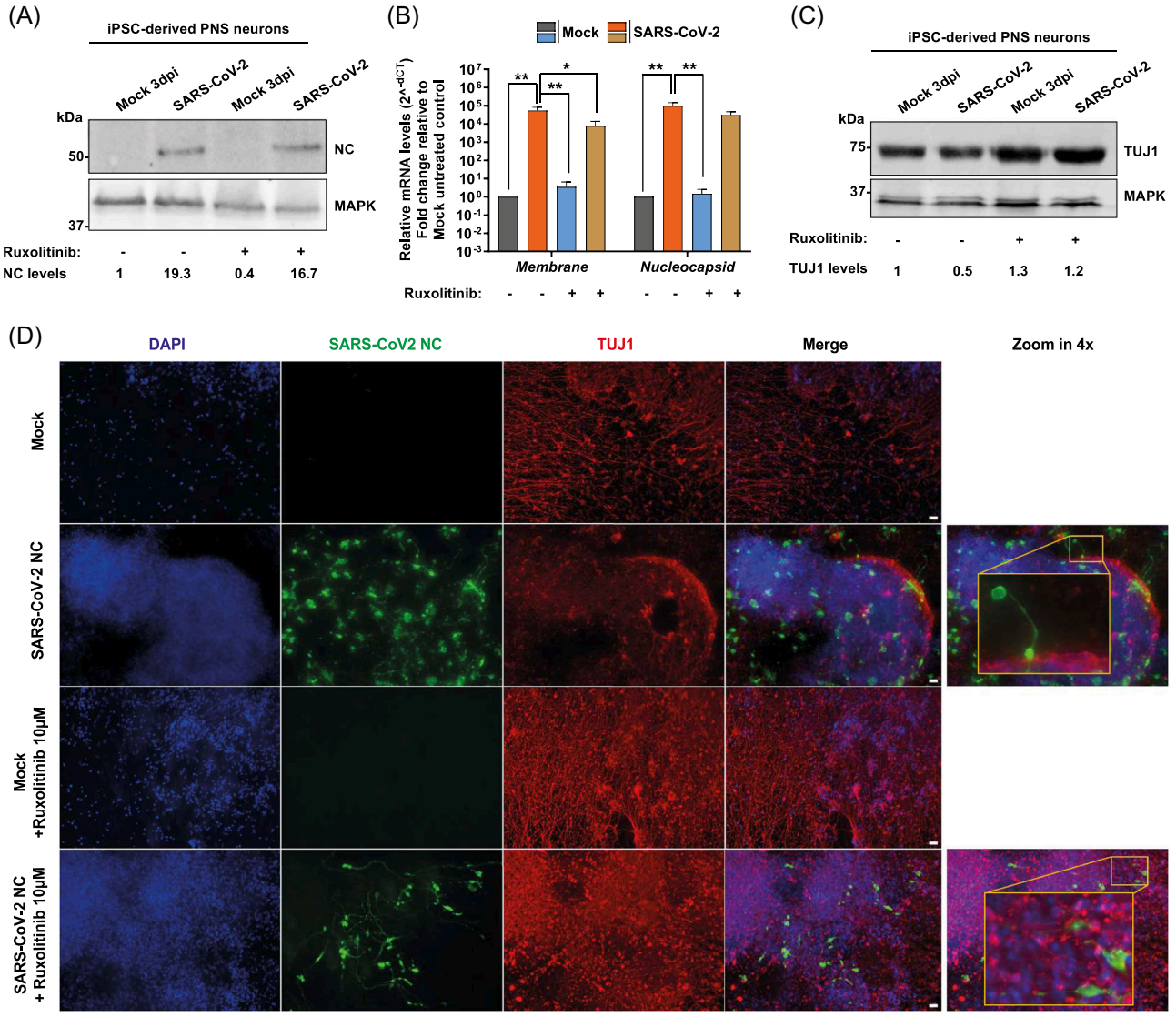

FIGURE 4 SARS-CoV-2 efficiently infects PNS neurons and induces robust type III IFN responses and ISG expression. (A) Immunoblot showing SARS-CoV-2 NC and MAPK in PNS neurons lysed at 3 dpi. NC levels were measured relative to MAPK using ImageJ. A representative blot is shown from three independent experiments. (B) Graph showing relative expression of SARS-CoV-2 *Membrane* and *Nucleocapsid* mRNA in PNS neurons at 3 dpi. (C) Immunoblot showing TUJ1 and MAPK in cell lysates of PNS neurons at 3 dpi. TUJ1 levels were measured relative to MAPK using ImageJ. One representative blot, out of three independent ones, is shown. (D) Immunofluorescence of PNS neurons fixed at 3 dpi and stained with anti-SARS-CoV-2 NC, anti-TUJ1, and DAPI. The right panels show a zoom in of 4x, applied using ImageJ. Scale bar = 100 μm; amplification: ×20. (E, G, I) Graphs showing relative expression of host genes in PNS neurons at 3 dpi. (F) Protein concentrations of released cytokines determined by ELISA. (H) Immunoblot showing ISG15 and MAPK in lysates of PNS neurons at 3 dpi. ISG15 levels were measured relative to MAPK using ImageJ. One representative blot, out of three independent ones, is shown. (J) Protein concentrations of released cytokines determined by cytometric bead array multiplex analysis in the supernatant of infected PNS neurons. In all immunoblots, the numbers at the bottom of the blot represent the fold-change to mock-infected, untreated control. In all graphs showing gene expression, this was quantified by RT-qPCR and set relative to β-actin. Fold-change is relative to mock-infected, untreated control. In all graphs, error bars represent standard deviation of the arithmetic mean from three independent experiments. Statistical analyses for all experiments were determined using one-way ANOVA followed by the Dunnetts multiple comparison posttest. *$p < 0.03$; **$p < 0.002$; ***$p < 0.0002$; ****$p < 0.0001$; not significant comparisons are not indicated. IFN, interferon; PNS, peripheral nervous system; SARS-CoV-2, severe acute respiratory coronavirus 2.

neurons, which significantly increased *IFN-λ1* and *IFN-λ2* gene expression and released IFN-λ1 protein, compared to mock-infected cells (Figure 4E,F). Addition of Ruxolitinib decreased the mRNA and protein levels of IFN-λ1 in SARS-CoV-2-infected cells, while it increased the protein amount of IFN-λ2 in the mock-infected cells (Figure 4E,F). Infection did not induce type I IFN and decreased slightly the expression of type II IFN, without affecting the protein level of IFN-γ (Figure 4E,J). We observed upregulation of *ISG15* and *Mx1* and downregulation of *IFIT1*, and *STAT2* mRNA levels in infected PNS neurons compared to mock-infected cells (Figure 4G). The increased ISG15 expression was also confirmed at the protein level (Figure 4H). The molecular weight of ISG15 was around 50 kDa,

10969071, 2024, 2, Downloaded from https://onlinelibrary.wiley.com/doi/10.1002/jmv.29455 by Deutsches Zentrum Für Neurodeg, Wiley Online Library on [19/02/2024]. See the Terms and Conditions (https://onlinelibrary.wiley.com/terms-and-conditions) on Wiley Online Library for rules of use; OA articles are governed by the applicable Creative Commons License

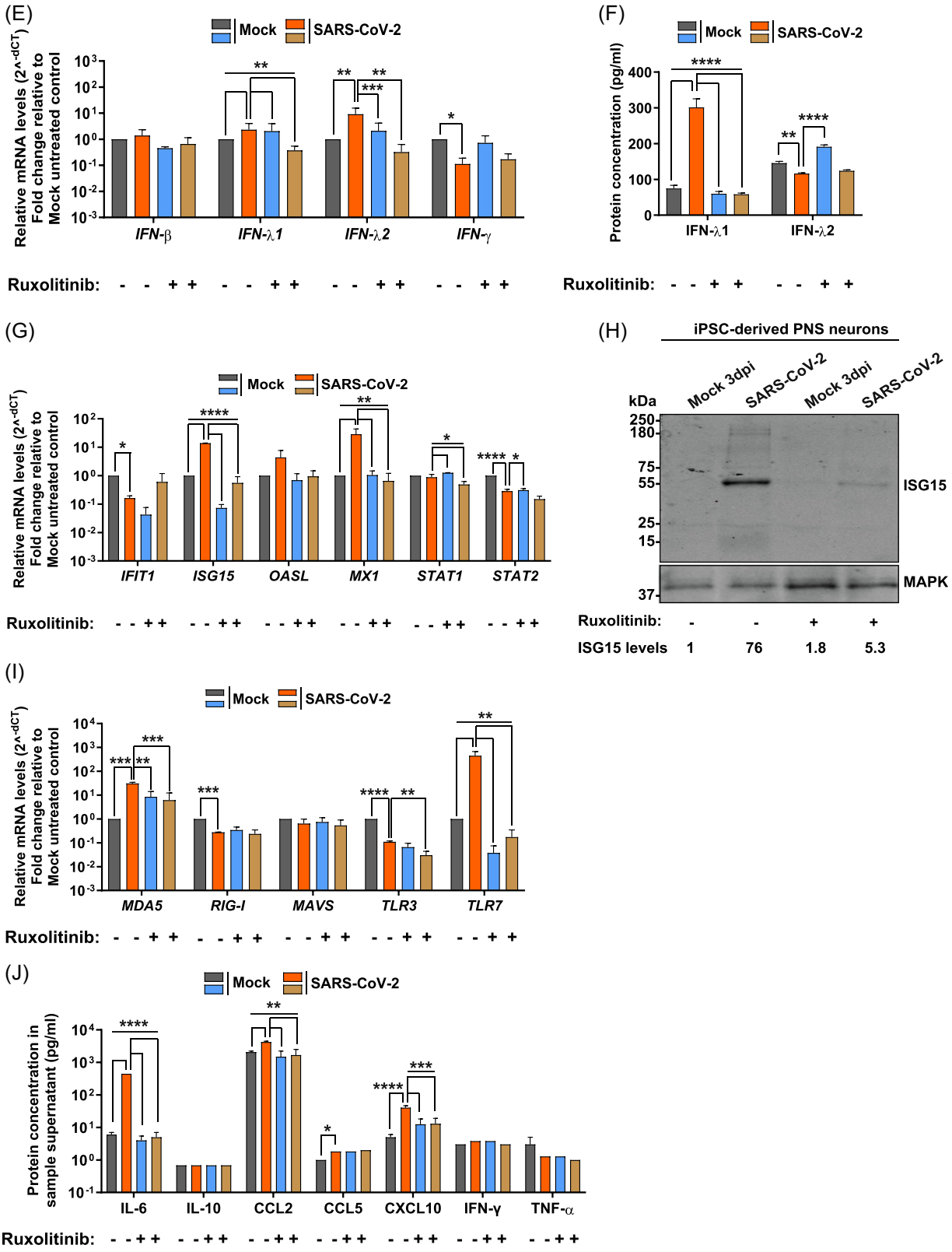

FIGURE 4 (Continued).

instead of 15 kDa, suggesting that it was ISGylated or associated with conjugates rather than the free form of ISG15 (Figure 4H). Ruxolitinib reduced ISG gene expression in the SARS-CoV-2-infected cells to basal levels (Figure 4E,G).

Next, we evaluated the expression levels of RNA sensors in PNS neurons upon SARS-CoV-2 infection. Infection increased *MDA5* and *TLR7* transcripts and decreased those of *RIG-I* and *TLR3*, suggesting a relevance for these sensors in the recognition of SARS-CoV-2 in PNS

10969071, 2024, 2, Downloaded from https://onlinelibrary.wiley.com/doi/10.1002/jmv.29455 by Deutsches Zentrum Für Neurologe, Wiley Online Library on [19/02/2024]. See the Terms and Conditions (https://onlinelibrary.wiley.com/terms-and-conditions) on Wiley Online Library for rules of use; OA articles are governed by the applicable Creative Commons License

neurons (Figure 4I). Analysis of the cytokine/chemokine profile showed an increase in IL-6, CCL2, CCL5, and CXCL10 in SARS-CoV-2-infected PNS neurons compared to mock-treated cells, revealing a phenotype that resembles the cytokine storm observed in severe COVID-19 patients (Figure 4J). Addition of Ruxolitinib inhibited the increase in cytokine expression observed during SARS-CoV-2 infection of iPSC-derived PNS neurons (Figure 4J).

Overall, these results showed that SARS-CoV-2 productively infects iPSC-derived PNS neurons, leading to high innate immune response and loss of β-III-tubulin, which was less pronounced when the JAK/STAT pathway was inhibited.

3.5 | SARS-CoV-2 infection of PNS neurons increased the expression of genes involved in axonal degeneration

To study whether the activation of innate immune responses and the induction of stress pathways could lead to neuronal damage, we infected PNS neurons with SARS-CoV-2 in the presence or absence of Ruxolitinib and analyzed the expression of genes related to the UPR pathway. Infection resulted in higher expression of *ATF4*, and no significant changes in transcription of *CHOP*, *BiP*, and *GRP94* (Figure 5A,B). Treatment with Ruxolitinib decreased the expression of *ATF4* and increased that of *CHOP* in the infected cells, supporting the hypothesis that the JAK/STAT pathway might play a role in the UPR in PNS neurons (Figure 5A).

To further explore the reduced level of β-III-tubulin in PNS neurons upon SARS-CoV-2 infection, we analyzed the expression level of genes involved in axonal degeneration. SARM1 mRNA and protein levels were significantly increased, pointing to its potential role in axonal degeneration in PNS neurons upon infection with SARS-CoV-2 (Figure 5C,D). Additionally, *MAP2* transcript levels were significantly reduced in SARS-CoV-2-infected cells compared to the mock-infected cells (Figure 5C). Interestingly, treatment with Ruxolitinib reverted the expression profile of *SARM1* and *MAP2*, suggesting a link between the innate immune response and neuronal damage in iPSC-derived PNS neurons infected with SARS-CoV-2 (Figure 5C,D). In addition, we observed significantly higher levels of released α-synuclein in the SN of PNS neurons infected with SARS-CoV-2 than in mock-infected neurons (Figure 5E).

In conclusion, our results indicate that iPSC-derived CNS neurons were more resistant than PNS neurons to SARS-CoV-2 infection. They also suggest that a combination of direct effects of SARS-CoV-2 and innate immune mechanisms induce neuronal damage in iPSC-derived human PNS neurons.

4 | DISCUSSION

Many COVID-19 patients suffer neurological complications. The protective role of the innate immune response of PNS and CNS neurons and its potential involvement in pathological outcomes upon SARS-CoV-2 infection are not well understood. Here, we addressed the role of the innate immune response upon SARS-CoV-2 infection of human iPSC-derived CNS and PNS neurons. Our results indicate that SARS-CoV-2 infection of PNS neurons induces neuronal damage through a mechanism that involves the innate immune response—potentially type III IFN—and SARM1.

Infection of CNS neurons—with properties of striatal MSNs—was very inefficient and did not change after inhibition of the JAK/STAT pathway. These results are similar to those obtained in postmortem human brains, which showed efficient infection of cortical neurons but not of MSNs.[23] Exposure of CNS neurons to SARS-CoV-2 did not lead to a robust innate immune response, ER stress response, or neuronal damage when investigating changes within the total cell population, probably due to the inefficient infection. The expression of IFN-β and IFN-λ2 increased upon infection, while that of IFN-γ decreased. Bauer and colleagues reported induction of IFN-λ2 and λ3 as well as IL-8 during abortive infection of iPSC-derived forebrain cortical neurons.[35]

Interestingly, in our hands, despite the low number of infected CNS neurons, BiP was upregulated at the mRNA and protein levels. BiP is a chaperone that acts like a sentinel of the ER and in homeostatic conditions maintains the UPR pathway inactive. Upon imbalance, such as a viral infection, BiP is no longer associated to the ER membrane, allowing activation of the UPR system to restore homeostasis. If homeostasis is not restored, apoptosis ensues.[65–67] There is a degree of controversy on the role of BiP during SARS-CoV-2 infection. One study showed that SARS-CoV-2 down-regulated BiP expression in primary differentiated human bronchial epithelial cells,[70] while others demonstrated the opposite: an increase of the UPR master regulator in the presence of SARS-CoV-2 in various cell types. The latter studies showed that BiP acts as a pro-viral factor, facilitating viral protein synthesis and particle release.[71,72] Additionally, other viruses incorporate BiP into viral particles to increase their maturation and support infection of new cells.[73] Moreover, BiP can act as an entry cofactor for several viruses, including SARS-CoV-2.[74] Imbalance of BiP has different consequences in the host: inhibition of BiP is detrimental, as the accumulation of misfolded proteins causes an exacerbated stress response. Increase of BiP keeps the UPR system inactive, protecting the host cells from undergoing apoptosis. Therefore, it is possible that BiP exerts a cytoprotective role and may contribute to the lack of cytopathic effects observed in CNS neurons upon SARS-CoV-2 infection.[75] Interestingly, Lindl et al., showed that an increase in the expression of BiP led to the reduction of CHOP transcripts,[76] as observed here in the iPSC-derived CNS neurons. Moreover, we observed also increased expression of *NMNAT2*, reduced levels of *SARM1*, higher level of the cytoskeletal protein β-III-tubulin and no increase in genes associated with neurodegeneration. Increased NMNAT2 levels are essential for axonal survival by blocking nicotinamide adenine dinucleotide (NAD+) depletion mediated by SARM1, which causes axonal degeneration.[77] This could also explain why CNS neurons are protected from neuronal degeneration during SARS-CoV-2 infection in our model.

10969071, 2024, 2, Downloaded from https://onlinelibrary.wiley.com/doi/10.1002/jmv.29455 by Deutsches Zentrum Für Neurologie, Wiley Online Library on [19/02/2024]. See the Terms and Conditions (https://onlinelibrary.wiley.com/terms-and-conditions) on Wiley Online Library for rules of use; OA articles are governed by the applicable Creative Commons License

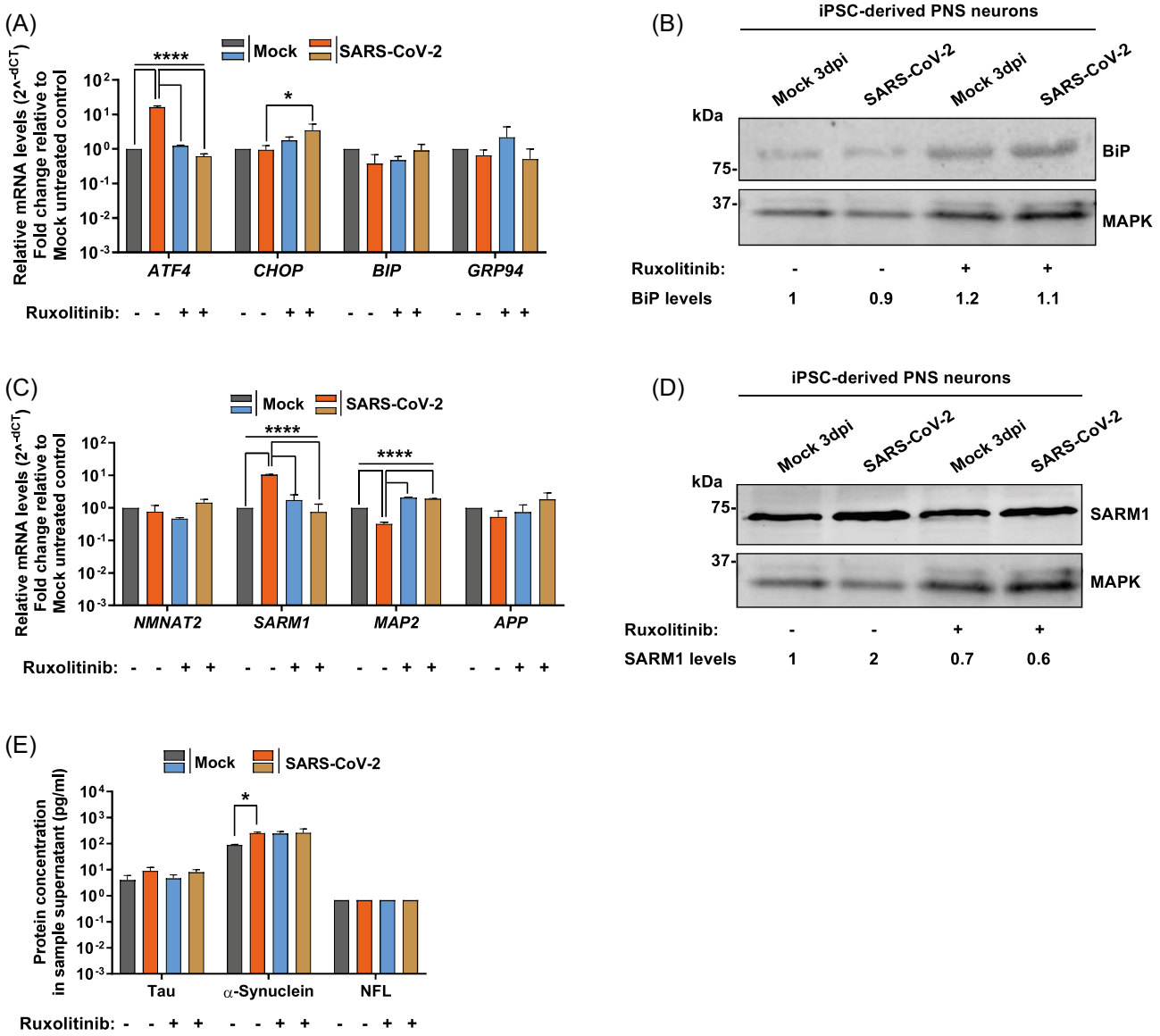

FIGURE 5 Stress response and axonal degeneration upon SARS-CoV-2 infection of PNS neurons. (A, C) Graphs showing relative expression of host genes in PNS neurons at 3 dpi. Gene expression was quantified by RT-qPCR and set to β-actin. Fold-change is relative to mock-infected, untreated control. (B, D) Immunoblots showing BiP (B), SARM1 (D), and MAPK (B, D) in cell lysates of PNS neurons at 3 dpi. Relative BiP and SARM1 levels were measured using ImageJ. The numbers at the bottom of the blot represent the fold-change to mock-infected, untreated control. One representative blot is shown from one experiment out of three independent ones. (E) Protein concentrations of released Tau, α-synuclein, and Neurofilament L (NFL) determined by cytometric bead array multiplex analysis. In all graphs, error bars represent standard deviation of the arithmetic mean from three independent experiments. Statistical analyses for all experiments were determined using one-way ANOVA followed by the Dunnetts multiple comparison posttest. *$p < 0.03$; **$p < 0.002$; ***$p < 0.0002$; ****$p < 0.0001$; not significant comparisons are not indicated. PNS, peripheral nervous system.

We cannot directly compare the results with the CNS and PNS neurons, since the infection of both neuronal subtypes was not performed simultaneously. However, we employed the same experimental conditions and internal controls in both sets of experiments. This allows us to reach relevant conclusions on the different outcomes of infection. Interestingly, SARS-CoV-2 infected a high number of human iPSC-derived PNS neurons despite low expression of *ACE2*, *TMPRSS2*, and *Nrp-1*. It is possible that SARS-CoV-2 infects PNS neurons through an ACE2-independent entry mechanism, as has been previously described for several cell lines and T lymphocytes.[78,79]

Infection of PNS neurons correlated with the initiation of a type III IFN response, expression of *Mx1*, *ISG15*, and proinflammatory cytokines like IL-6, CCL2, CCL5, and CXCL10 at 3 dpi. We did not detect induction of type I IFN response under such conditions, probably because this response occurs earlier and is less sustained than the induction of type III IFN.[80] The increased IFN-λ1 response in PNS neurons correlated with increased expression of *ATF4*, no

10969071, 2024, 2, Downloaded from https://onlinelibrary.wiley.com/doi/10.1002/jmv.29455 by Deutsches Zentrum Für Neurodeg, Wiley Online Library on [19/02/2024]. See the Terms and Conditions (https://onlinelibrary.wiley.com/terms-and-conditions) on Wiley Online Library for rules of use; OA articles are governed by the applicable Creative Commons License

changes in the master regulator of UPR (*BiP*), enhanced expression of neurodegeneration-related genes (*SARM1* and *APP*), an elevated level of proteins involved in neuronal damage (SARM1 and α-synuclein) and lower levels of β-III-tubulin, an essential protein maintaining the neuronal cytoskeleton. Studies performed in epithelial cells suggest a link between IFN-λ and induction of SARM1 and UPR.[81,82] The observed increased expression of *ATF4* together with lack of changes in *BiP* expression could contribute to apoptosis and autophagy,[83] and thereby neuronal damage in the human iPSC-derived PNS neurons. Interestingly, inhibition of the JAK/STAT pathway reverted this phenotype in PNS neurons, suggesting a link between the innate immune response, ER stress response, expression of SARM1, and neurodegenerative processes in the context of SARS-CoV-2 infection. Ruxolitinib also slightly decreased SARS-CoV-2 gene expression, and this could also explain the lower cytopathic effect observed.

Neurons express IFN-λ and its receptor.[38] However, the potential link between type III IFN and neuronal damage during infection is understudied. The higher expression of IFN-λ1 in PNS neurons correlated with upregulation of *ISG15* and *Mx1*. ISGylation of ISG15 combined with high level of Mx1 were detected in peripheral mononuclear cells in symptomatic COVID-19 patients.[84] Moreover, upregulation of ISG15 and its potential ISGylation could contribute to aberrant protein degradation, promoting the accumulation of cellular proteins such as APP, and to increased autophagy, contributing to neurodegenerative diseases.[85]

SARM1 is both necessary and sufficient to initiate axonal degeneration,[53,55] the first stage of many neurodegenerative diseases, including peripheral neuropathies.[86,87] SARM1 is inactive in healthy axons but becomes active upon injury or insult, including infection, due to depletion of NMNAT2.[68] NMNAT2 promotes the synthesis of NAD+ through an enzymatic reaction of nicotinamide mononucleotide and adenosine triphosphate. SARM1 activation leads to hydrolysis of NAD into Nam, calcium influx, and activation of calpains that degrade cytoskeletal proteins such as β-III-tubulin, causing neurite degeneration.[88–91] Upon infection of PNS neurons with SARS-CoV-2, there was a JAK/STAT-dependent activation of SARM1 that correlated with lower levels of β-III-tubulin and increase of neurodegenerative markers.

SARM1 plays different roles in infection with different viruses. For instance, SARM1 knock out mice responded as wild type littermates to influenza, but were protected from neurodegeneration after CNS infection with vesicular stomatitis virus.[54] This correlated with reduced levels of cytokine production in the CNS.[54] On the contrary, mice lacking SARM1 expression were more susceptible to West Nile virus infection.[92] Sundaramoorthy showed that SARM1 activation acts as a defense mechanism to inhibit rabies virus infection of neuronal cell bodies.[50] Our results also indicate a link between the innate immune response and SARM1 upon SARS-CoV-2 infection. The increased expression of SARM1 and reduced levels of cytoskeletal proteins upon SARS-CoV-2 infection of PNS neurons could lead to axonal degeneration and nerve fiber loss, causing neurological disease, as observed in some COVID-19 patients.[11,17,18]

In conclusion, we show that SARS-CoV-2 only infected a reduced number of iPSC-derived CNS neurons and did not lead to a robust innate immune response, nor to a neurodegenerative phenotype. In contrast, SARS-CoV-2 efficiently infected human iPSC-derived PNS neurons, triggering the innate immune response that was partially responsible for the neurodegenerative-like phenotype. The pathological cytokine responses were characterized by high levels of IFN-λ1, expression of ISGs, cytokines, ER-stress genes, and genes involved in triggering neuronal damage, like SARM1, and accumulation of cellular proteins responsible for neuronal damage such as α-synuclein. In the iPSC-derived human PNS neurons employed here, blocking the JAK/STAT pathway ameliorated the neuronal damage phenotype through decreasing *SARM1* and *ATF4* expression levels, and reducing SARM1 protein level. This was accompanied by an increase in β-III-tubulin and *MAP2*, linking the innate immune response and neuronal damage in this model. A considerable number of COVID-19 patients suffers from many symptoms associated with neuronal dysfunction in the PNS, including loss of innervation and increased neuropathy.[17,18] Our results cannot explain the broad range of different neurological symptoms from which COVID-19 patients suffer, but they provide a model to further explore the role of the infection and the innate immune response in the neuronal pathology and to test future preventive or therapeutic strategies.

AUTHOR CONTRIBUTIONS

Vania Passos and Abel Viejo-Borbolla conceptualized the project. Ulrich Kalinke, Günter Höglinger, Gisa Gerold, Florian Wegner, and Abel Viejo-Borbolla supervised the project. Vania Passos performed and analyzed most experiments. Lisa M. Henkel, Jiayi Wang, Francisco J. Zapatero-Belinchón, Rebecca Möller, Guorong Sun, Inken Waltl, Talia Schneider, Amelie Wachs, and Birgit Ritter contributed to the experiments. Kai A. Kropp contributed to data analysis. Shuyong Zhu, Michela Deleidi, and Thomas F. Schulz provided relevant resources and methodology. Abel Viejo-Borbolla obtained funding. Vania Passos and Abel Viejo-Borbolla wrote the original draft and together with Michela Deleidi, Shuyong Zhu, Ulrich Kalinke, Günter Höglinger, Gisa Gerold, and Florian Wegner reviewed it and edited it.

ACKNOWLEDGMENTS

We thank Ulrich Martin and Alexandra Haase (LEBAO, Hannover Medical School, Germany) for providing the iPSC line to differentiate PNS neurons. We thank Stephanie Pfänder (Ruhr University Bochum) for scientific advice and protocols. We are thankful to Saskia Stein (Institute of Virology, Hannover Medical School, Germany) for help during the introduction to the BSL3 laboratory. We thank Arnaud Carpentier (Twincore, Hannover), Carina Jürgens (Institute of Virology, Hannover Medical School, Germany), and Stephanie Pfänder for providing primer sequences. We are thankful to Thomas Pietschmann for providing the UV-inactivated virus and the Vero cells. We thank Beate Sodeik (Institute of Virology, Hannover Medical School, Germany) for providing the anti-ISG15 antibody. We thank Ruth Knorr of the BSL3 facility at Hannover Medical

10969071, 2024, 2, Downloaded from https://onlinelibrary.wiley.com/doi/10.1002/jmv.29455 by Deutsches Zentrum Für Neurologe, Wiley Online Library on [19/02/2024]. See the Terms and Conditions (https://onlinelibrary.wiley.com/terms-and-conditions) on Wiley Online Library for rules of use; OA articles are governed by the applicable Creative Commons License

School as well as Katja Branitzki-Heinemann and Maren von Köckritz-Blickwede of the BSL3 facility at University of Veterinary Medicine Hannover for their continuous support. We thank Julie Ann Sheldon, Twincore, Hannover for critical proofreading. This work was supported by the Deutsche Forschungsgemeinschaft (DFG, German Research Foundation) COVID-19 Focus, project number 458632757 awarded to A. V.-B. (VI 762/2-1) and by the Deutsche Forschungsgemeinschaft (DFG, German Research Foundation) under Germany's Excellence Strategy–EXC 2155–project number 390874280 (https://www.resist-cluster.de/en/). K. K. was funded by the Deutsche Forschungsgemeinschaft (DFG, German Research Foundation)–SFB 900/3–project number 158989968 to A. V.-B. (TPB9, https://www.sfb900.de/en/). J. W. and G. S. were funded by CSC Scholarships (No. 201908370216 and 201808230268, respectively) and were supported by the Hannover Biomedical Research School (HBRS) and the Center for Infection Biology (ZIB). Open Access funding enabled and organized by Projekt DEAL.

CONFLICT OF INTEREST STATEMENT

The authors declare no conflict of interest.

DATA AVAILABILITY STATEMENT

The data that support the findings of this study are available from the corresponding author upon reasonable request.

ORCID

Francisco J. Zapatero-Belinchón http://orcid.org/0000-0002-2751-8411
Guorong Sun http://orcid.org/0000-0001-7549-7304
Inken Waltl http://orcid.org/0000-0001-7518-1035
Talia Schneider http://orcid.org/0000-0002-8796-0404
Kai A. Kropp http://orcid.org/0000-0001-8505-3440
Michela Deleidi http://orcid.org/0000-0003-0357-0124
Ulrich Kalinke http://orcid.org/0000-0003-0503-9564
Thomas F. Schulz http://orcid.org/0000-0001-8792-5345
Günter Höglinger http://orcid.org/0000-0001-7587-6187
Gisa Gerold http://orcid.org/0000-0002-1326-5038
Abel Viejo-Borbolla http://orcid.org/0000-0001-6395-4010

REFERENCES

1. Paterson RW, Brown RL, Benjamin L, et al. The emerging spectrum of COVID-19 neurology: clinical, radiological and laboratory findings. *Brain*. 2020;143(10):3104-3120.
2. Alipoor SD, Jamaati H, Tabarsi P, Mortaz E. Immunopathogenesis of pneumonia in COVID-19. *Tanaffos*. 2020;19(2):79-82.
3. Taquet M, Geddes JR, Husain M, Luciano S, Harrison PJ. 6-month neurological and psychiatric outcomes in 236 379 survivors of COVID-19: a retrospective cohort study using electronic health records. *Lancet Psychiatr*. 2021;8(5):416-427.
4. Mao L, Jin H, Wang M, et al. Neurologic manifestations of hospitalized patients with coronavirus disease 2019 in Wuhan, China. *JAMA Neurol*. 2020;77(6):683-690.
5. Zanin L, Saraceno G, Panciani PP, et al. SARS-CoV-2 can induce brain and spine demyelinating lesions. *Acta Neurochir*. 2020;162(7):1491-1494.
6. Helms J, Kremer S, Merdji H, et al. Neurologic features in severe SARS-CoV-2 infection. *N Engl J Med*. 2020;382(23):2268-2270.
7. Politi LS, Salsano E, Grimaldi M. Magnetic resonance imaging alteration of the brain in a patient with coronavirus disease 2019 (COVID-19) and anosmia. *JAMA Neurol*. 2020;77(8):1028-1029.
8. McFarland AJ, Yousuf MS, Shiers S, Price TJ. Neurobiology of SARS-CoV-2 interactions with the peripheral nervous system: implications for COVID-19 and pain. *PAIN Reports*. 2021;6(1):e885.
9. Andalib S, Biller J, Di Napoli M, et al. Peripheral nervous system manifestations associated with COVID-19. *Curr Neurol Neurosci Rep*. 2021;21(3):9.
10. Zhao H, Shen D, Zhou H, Liu J, Chen S. Guillain-Barré syndrome associated with SARS-CoV-2 infection: causality or coincidence? *Lancet Neurol*. 2020;19(5):383-384.
11. Abdelnour L, Eltahir Abdalla M, Babiker S. COVID 19 infection presenting as motor peripheral neuropathy. *J Formos Med Assoc*. 2020;119(6):1119-1120.
12. Romero-Sánchez CM, Díaz-Maroto I, Fernández-Díaz E, et al. Neurologic manifestations in hospitalized patients with COVID-19: the ALBACOVID registry. *Neurology*. 2020;95(8):e1060-e1070.
13. Huber M, Rogozinski S, Puppe W, et al. Postinfectious onset of myasthenia gravis in a COVID-19 patient. *Front Neurol*. 2020;11:576153. doi:10.3389/fneur.2020.576153
14. Stefanou MI, Palaiodimou L, Bakola E, et al. Neurological manifestations of long-COVID syndrome: a narrative review. *Ther Adv Chronic Dis*. 2022;13:20406223221076890.
15. Ali ST, Kang AK, Patel TR, et al. Evolution of neurologic symptoms in non-hospitalized COVID-19 long haulers. *Ann Clin Transl Neurol*. 2022;9(7):950-961.
16. Spudich S, Nath A. Nervous system consequences of COVID-19. *Science*. 2022;375(6578):267-269.
17. Bitirgen G, Korkmaz C, Zamani A, et al. Corneal confocal microscopy identifies corneal nerve fibre loss and increased dendritic cells in patients with long COVID. *Br J Ophthalmol*. 2022;106(12):1635-1641. doi:10.1136/bjophthalmol-2021-319450
18. Oaklander AL, Mills AJ, Kelley M, et al. Peripheral neuropathy evaluations of patients with prolonged long COVID. *Neurol Neuroimmunol Neuroinflammation*. 2022;9(3):e1146. doi:10.1212/NXI.0000000000001146
19. Moriguchi T, Harii N, Goto J, et al. A first case of meningitis/encephalitis associated with SARS-Coronavirus-2. *Int J Infect Dis*. 2020;94:55-58.
20. Puelles VG, Lütgehetmann M, Lindenmeyer MT, et al. Multiorgan and renal tropism of SARS-CoV-2. *N Engl J Med*. 2020;383(6):590-592.
21. Solomon IH, Normandin E, Bhattacharyya S, et al. Neuropathological features of Covid-19. *N Engl J Med*. 2020;383(10):989-992.
22. Wu Y, Xu X, Chen Z, et al. Nervous system involvement after infection with COVID-19 and other coronaviruses. *Brain Behav Immun*. 2020;87:18-22.
23. Song E, Zhang C, Israelow B, et al. Neuroinvasion of SARS-CoV-2 in human and mouse brain. *J Exp Med*. 2021;218:3.
24. Farhadian S, Glick LR, Vogels CBF, et al. Acute encephalopathy with elevated CSF inflammatory markers as the initial presentation of COVID-19. *BMC Neurol*. 2020;20(1):248.
25. Koenigsknecht-Talboo J, Landreth GE. Microglial phagocytosis induced by fibrillar β-amyloid and IgGs are differentially regulated by proinflammatory cytokines. *J Neurosci*. 2005;25(36):8240-8249.
26. Nagu P, Parashar A, Behl T, Mehta V. CNS implications of COVID-19: a comprehensive review. *Rev Neurosci*. 2021;32(2):219-234.
27. Magliozzi R, Howell OW, Nicholas R, et al. Inflammatory intrathecal profiles and cortical damage in multiple sclerosis. *Ann Neurol*. 2018;83(4):739-755.

10969071, 2024, 2, Downloaded from https://onlinelibrary.wiley.com/doi/10.1002/jmv.29455 by Deutsches Zentrum Für Neurologie, Wiley Online Library on [19/02/2024]. See the Terms and Conditions (https://onlinelibrary.wiley.com/terms-and-conditions) on Wiley Online Library for rules of use; OA articles are governed by the applicable Creative Commons License

28. Schwarzschild MA. Serum urate as a predictor of clinical and radiographic progression in Parkinson disease. *Arch Neurol*. 2008;65(6):716-723.
29. Pilotto A, Masciocchi S, Volonghi I, et al. Severe acute respiratory syndrome coronavirus 2 (SARS-CoV-2) encephalitis is a cytokine release syndrome: evidences from cerebrospinal fluid analyses. *Clin Infect Dis*. 2021;73(9):e3019-e3026.
30. Ramani A, Müller L, Ostermann PN, et al. SARS-CoV-2 targets neurons of 3D human brain organoids. *EMBO J*. 2020;39(20):e106230.
31. Bullen CK, Hogberg HT, Bahadirli-Talbott A, et al. Infectability of human BrainSphere neurons suggests neurotropism of SARS-CoV-2. *ALTEX*. 2020;37(4):665-671.
32. Jacob F, Pather SR, Huang WK, et al. Human pluripotent stem cell-derived neural cells and brain organoids reveal SARS-CoV-2 neurotropism predominates in choroid plexus epithelium. *Cell Stem Cell*. 2020;27(6):937-950.
33. McMahon CL, Staples H, Gazi M, Carrion R, Hsieh J. SARS-CoV-2 targets glial cells in human cortical organoids. *Stem Cell Reports*. 2021;16(5):1156-1164.
34. Pellegrini L, Albecka A, Mallery DL, et al. SARS-CoV-2 infects the brain choroid plexus and disrupts the blood-CSF barrier in human brain organoids. *Cell Stem Cell*. 2020;27(6):951-961.
35. Bauer L, Lendemeijer B, Leijten L, et al. Replication kinetics, cell tropism, and associated immune responses in SARS-CoV-2- and H5N1 virus-infected human induced pluripotent stem cell-derived neural models. *mSphere*. 2021;6(3):e0027021.
36. Tiwari SK, Wang S, Smith D, Carlin AF, Rana TM. Revealing tissue-specific SARS-CoV-2 infection and host responses using human stem cell-derived lung and cerebral organoids. *Stem Cell Rep*. 2021;16(3):437-445.
37. Lyoo KS, Kim HM, Lee B, et al. Direct neuronal infection of SARS-CoV-2 reveals cellular and molecular pathology of chemosensory impairment of COVID-19 patients. *Emerg Microbes Infect*. 2022;11(1):407-412.
38. Zhou L, Wang X, Wang YJ, et al. Activation of Toll-like receptor-3 induces interferon-λ expression in human neuronal cells. *Neuroscience*. 2009;159(2):629-637.
39. Gao D, Ciancanelli MJ, Zhang P, et al. TLR3 controls constitutive IFN-beta antiviral immunity in human fibroblasts and cortical neurons. *J Clin Invest*. 2021;131(1):e134529. doi:10.1172/JCI134529
40. Li J, Hu S, Zhou L, et al. Interferon lambda inhibits herpes simplex virus type I infection of human astrocytes and neurons. *GLIA*. 2011;59(1):58-67.
41. Chhatbar C, Detje CN, Grabski E, et al. Type I interferon receptor signaling of neurons and astrocytes regulates microglia activation during viral encephalitis. *Cell Rep*. 2018;25(1):118-129.
42. Cavanaugh SE, Holmgren AM, Rall GF. Homeostatic interferon expression in neurons is sufficient for early control of viral infection. *J Neuroimmunol*. 2015;279:11-19.
43. Delhaye S, Paul S, Blakqori G, et al. Neurons produce type I interferon during viral encephalitis. *Proc Natl Acad Sci*. 2006;103(20):7835-7840.
44. Ghita L, Spanier J, Chhatbar C, et al. MyD88 signaling by neurons induces chemokines that recruit protective leukocytes to the virus-infected CNS. *Sci Immunol*. 2021;6(60):eabc9165. doi:10.1126/sciimmunol.abc9165
45. Mori I, Nishiyama Y, Yokochi T, Kimura Y. Virus-induced neuronal apoptosis as pathological and protective responses of the host. *Rev Med Virol*. 2004;14(4):209-216.
46. Crawford CL, Antoniou C, Komarek L, et al. SARM1 depletion slows axon degeneration in a CNS model of neurotropic viral infection. *Front Mol Neurosci*. 2022;15:860410.
47. Tsunoda I. Axonal degeneration as a self-destructive defense mechanism against neurotropic virus infection. *Future Virol*. 2008;3(6):579-593.
48. Chawla K, Subramanian G, Rahman T, et al. Autophagy in virus infection: a race between host immune response and viral antagonism. *Immuno*. 2022;2(1):153-169.
49. Yordy B, Iijima N, Huttner A, Leib D, Iwasaki A. A neuron-specific role for autophagy in antiviral defense against herpes simplex virus. *Cell Host Microbe*. 2012;12(3):334-345.
50. Sundaramoorthy V, Green D, Locke K, O'Brien CM, Dearnley M, Bingham J. Novel role of SARM1 mediated axonal degeneration in the pathogenesis of rabies. *PLoS Pathog*. 2020;16(2):e1008343.
51. Alfano C, Gladwyn-Ng I, Couderc T, Lecuit M, Nguyen L. The unfolded protein response: a key player in zika virus-associated congenital microcephaly. *Front Cell Neurosci*. 2019;13:94.
52. Medigeshi GR, Lancaster AM, Hirsch AJ, et al. West Nile virus infection activates the unfolded protein response, leading to CHOP induction and apoptosis. *J Virol*. 2007;81(20):10849-10860.
53. Gerdts J, Brace EJ, Sasaki Y, DiAntonio A, Milbrandt J. SARM1 activation triggers axon degeneration locally via NAD(+) destruction. *Science*. 2015;348(6233):453-457.
54. Hou YJ, Banerjee R, Thomas B, et al. SARM is required for neuronal injury and cytokine production in response to central nervous system viral infection. *J Immunol*. 2013;191(2):875-883.
55. Osterloh JM, Yang J, Rooney TM, et al. dSarm/Sarm1 is required for activation of an injury-induced axon death pathway. *Science*. 2012;337(6093):481-484.
56. Zhu S, Stanslowsky N, Fernández-Trillo J, et al. Generation of hiPSC-derived low threshold mechanoreceptors containing axonal termini resembling bulbous sensory nerve endings and expressing Piezo1 and Piezo2. *Stem Cell Res*. 2021;56:102535.
57. Kutschenko A, Staege S, Grütz K, et al. Functional and molecular properties of DYT-SGCE myoclonus-dystonia patient-derived striatal medium spiny neurons. *Int J Mol Sci*. 2021;22(7):3565.
58. Naujock M, Stanslowsky N, Reinhardt P, et al. Molecular and functional analyses of motor neurons generated from human cord-blood-derived induced pluripotent stem cells. *Stem Cells Dev*. 2014;23(24):3011-3020.
59. Schöndorf DC, Aureli M, McAllister FE, et al. iPSC-derived neurons from GBA1-associated Parkinson's disease patients show autophagic defects and impaired calcium homeostasis. *Nat Commun*. 2014;5:4028.
60. Hoffmann M, Kleine-Weber H, Schroeder S, et al. SARS-CoV-2 cell entry depends on ACE2 and TMPRSS2 and is blocked by a clinically proven protease inhibitor. *Cell*. 2020;181(2):271-280.
61. Zhou P, Yang XL, Wang XG, et al. A pneumonia outbreak associated with a new coronavirus of probable bat origin. *Nature*. 2020;579(7798):270-273.
62. Cantuti-Castelvetri L, Ojha R, Pedro LD, et al. Neuropilin-1 facilitates SARS-CoV-2 cell entry and infectivity. *Science*. 2020;370(6518):856-860.
63. Daly JL, Simonetti B, Klein K, et al. Neuropilin-1 is a host factor for SARS-CoV-2 infection. *Science*. 2020;370(6518):861-865.
64. Kong W, Montano M, Corley MJ, et al. Neuropilin-1 mediates SARS-CoV-2 infection of astrocytes in brain organoids, inducing inflammation leading to dysfunction and death of neurons. *mBio*. 2022;13:e0230822.
65. Read A, Schröder M. The unfolded protein response: an overview. *Biology*. 2021;10(5):384.
66. Pitale PM, Gorbatyuk O, Gorbatyuk M. Neurodegeneration: keeping ATF4 on a tight leash. *Front Cell Neurosci*. 2017;11:410.
67. Zhu G, Lee AS. Role of the unfolded protein response, GRP78 and GRP94 in organ homeostasis. *J Cell Physiol*. 2015;230(7):1413-1420.

10969071, 2024, 2, Downloaded from https://onlinelibrary.wiley.com/doi/10.1002/jmv.29455 by Deutsches Zentrum Für Neurologe, Wiley Online Library on [19/02/2024]. See the Terms and Conditions (https://onlinelibrary.wiley.com/terms-and-conditions) on Wiley Online Library for rules of use; OA articles are governed by the applicable Creative Commons License

68. Figley MD, Gu W, Nanson JD, et al. SARM1 is a metabolic sensor activated by an increased NMN/NAD(+) ratio to trigger axon degeneration. *Neuron*. 2021;109(7):1118-1136.
69. Hendershot LM. The ER function BiP is a master regulator of ER function. *Mount Sinai J Med, New York*. 2004;71(5):289-297.
70. Shaban MS, Müller C, Mayr-Buro C, et al. Multi-level inhibition of coronavirus replication by chemical ER stress. *Nat Commun*. 2021;12(1):5536.
71. Shin WJ, Ha DP, Machida K, Lee AS. The stress-inducible ER chaperone GRP78/BiP is upregulated during SARS-CoV-2 infection and acts as a pro-viral protein. *Nat Commun*. 2022;13(1):6551.
72. Ha DP, Van Krieken R, Carlos AJ, Lee AS. The stress-inducible molecular chaperone GRP78 as potential therapeutic target for coronavirus infection. *J Infect*. 2020;81(3):452-482.
73. Wu YP, Chang CM, Hung CY, et al. Japanese encephalitis virus co-opts the ER-stress response protein GRP78 for viral infectivity. *Virol J*. 2011;8:128.
74. Carlos AJ, Ha DP, Yeh DW, et al. The chaperone GRP78 is a host auxiliary factor for SARS-CoV-2 and GRP78 depleting antibody blocks viral entry and infection. *J Biol Chem*. 2021;296:100759.
75. Lewy TG, Grabowski JM, Bloom ME. BiP: master regulator of the unfolded protein response and crucial factor in flavivirus biology. *Yale J Biol Med*. 2017;90(2):291-300.
76. Lindl KA, Akay C, Wang Y, White MG, Jordan-Sciutto KL. Expression of the endoplasmic reticulum stress response marker, BiP, in the central nervous system of HIV-positive individuals. *Neuropathol Appl Neurobiol*. 2007;33(6):658-669.
77. Walker LJ, Summers DW, Sasaki Y, Brace E, Milbrandt J, DiAntonio A. MAPK signaling promotes axonal degeneration by speeding the turnover of the axonal maintenance factor NMNAT2. *eLife*. 2017;6:e22540. doi:10.7554/eLife.22540
78. Hoffmann M, Sidarovich A, Arora P, et al. Evidence for an ACE2-independent entry pathway that can protect from neutralization by an antibody used for COVID-19 therapy. *mBio*. 2022;13:e0036422.
79. Shen XR, Geng R, Li Q, et al. ACE2-independent infection of T lymphocytes by SARS-CoV-2. *Signal Transduct Target Ther*. 2022;7(1):83.
80. Lazear HM, Schoggins JW, Diamond MS. Shared and distinct functions of type I and type III interferons. *Immunity*. 2019;50(4):907-923.
81. Kanda T, Jiang X, Nakamoto S, et al. Different effects of three interferons L on Toll-like receptor-related gene expression in HepG2 cells. *Cytokine*. 2013;64(2):577-583.
82. Chen Q, Coto-Llerena M, Suslov A, et al. Interferon lambda 4 impairs hepatitis C viral antigen presentation and attenuates T cell responses. *Nat Commun*. 2021;12(1):4882.
83. Matsumoto H, Miyazaki S, Matsuyama S, et al. Selection of autophagy or apoptosis in cells exposed to ER-stress depends on ATF4 expression pattern with or without CHOP expression. *Biol Open*. 2013;2(10):1084-1090.
84. Schwartzenburg J, Reed R, Koul H, et al. ISGylation is increased in the peripheral blood mononuclear cells derived from symptomatic COVID-19 patients. *Exp Biol Med*. 2022;247(10):842-847.
85. Juncker M, Kim C, Reed R, Haas A, Schwartzenburg J, Desai S. ISG15 attenuates post-translational modifications of mitofusins and congression of damaged mitochondria in Ataxia Telangiectasia cells. *Biochimica et Biophysica Acta (BBA)-Mol Basis Dis*. 2021;1867(6):166102.
86. Geisler S, Doan RA, Strickland A, Huang X, Milbrandt J, DiAntonio A. Prevention of vincristine-induced peripheral neuropathy by genetic deletion of SARM1 in mice. *Brain*. 2016;139(Pt 12):3092-3108.
87. Geisler S, Huang SX, Strickland A, et al. Gene therapy targeting SARM1 blocks pathological axon degeneration in mice. *J Exp Med*. 2019;216(2):294-303.
88. Yang J, Weimer RM, Kallop D, et al. Regulation of axon degeneration after injury and in development by the endogenous calpain inhibitor calpastatin. *Neuron*. 2013;80(5):1175-1189.
89. Posmantur R, Kampfl A, Siman R, et al. A calpain inhibitor attenuates cortical cytoskeletal protein loss after experimental traumatic brain injury in the rat. *Neuroscience*. 1997;77(3):875-888.
90. Horsefield S, Burdett H, Zhang X, et al. NAD(+) cleavage activity by animal and plant TIR domains in cell death pathways. *Science*. 2019;365(6455):793-799.
91. Essuman K, Summers DW, Sasaki Y, Mao X, DiAntonio A, Milbrandt J. The SARM1 Toll/interleukin-1 receptor domain possesses intrinsic NAD(+) cleavage activity that promotes pathological axonal degeneration. *Neuron*. 2017;93(6):1334-1343.
92. Szretter KJ, Samuel MA, Gilfillan S, Fuchs A, Colonna M, Diamond MS. The immune adaptor molecule SARM modulates tumor necrosis factor alpha production and microglia activation in the brainstem and restricts West Nile virus pathogenesis. *J Virol*. 2009;83(18):9329-9338.

SUPPORTING INFORMATION

Additional supporting information can be found online in the Supporting Information section at the end of this article.n

How to cite this article: Passos V, Henkel LM, Wang J, et al. Innate immune response to SARS-CoV-2 infection contributes to neuronal damage in human iPSC-derived peripheral neurons. *J Med Virol*. 2024;96:e29455. doi:10.1002/jmv.29455

10969071, 2024, 2, Downloaded from https://onlinelibrary.wiley.com/doi/10.1002/jmv.29455 by Deutsches Zentrum Für Neurologe, Wiley Online Library on [19/02/2024]. See the Terms and Conditions (https://onlinelibrary.wiley.com/terms-and-conditions) on Wiley Online Library for rules of use; OA articles are governed by the applicable Creative Commons License